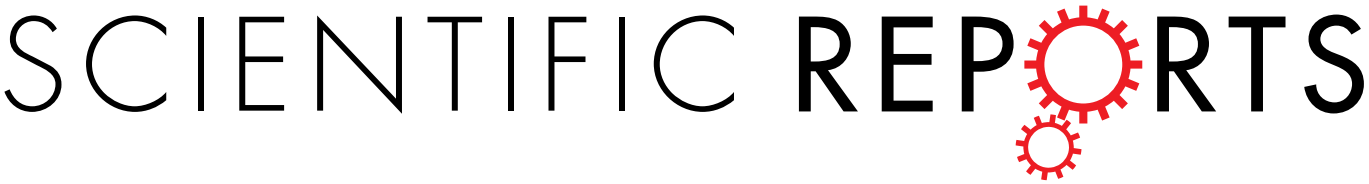

OPEN

Two-Dimensional Co_2S_2 monolayer with robust ferromagnetism

Yun Zhang[1], Jingman Pang[2], Meiguang Zhang[1], Xiao Gu[3] & Li Huang[4]

Received: 12 July 2017
Accepted: 6 November 2017
Published online: 22 November 2017

Design and synthesis of two-dimensional (2D) materials with robust intrinsic ferromagnetism is highly desirable due to their potential applications in spintronics devices. In this work, we identify a new 2D cobalt sulfide (Co_2S_2) material by using first-principles calculations and particle swarm optimization (PSO) global structure search. We show that the 2D Co_2S_2 is most stable in the litharge type tetragonal structure with space group of P4/nmm. The elastic constants, phonon spectrum, and molecular dynamics simulation confirm its mechanical, dynamical and thermal stability, respectively. It is also found that Co_2S_2 monolayer is a ferromagnetic metal with a Curie temperature up to 404 K. In addition, we propose a feasible procedure to synthesize the Co_2S_2 monolayer by chemically exfoliating from bulk $TlCo_2S_2$ phase.

Over the past decade, atomically thin two-dimensional (2D) materials have been extensively studied because they have many unique and fascinating physical and chemical properties compared to their bulk counterparts. Many efforts have been devoted to searching new 2D materials since the first report of the successful fabrication of graphene by Geim and Novoselov in 2004[1]. Recent theoretical and experimental studies have shown that many more 2D materials can be synthesized, such as hexagonal boron nitride (h-BN), transition-metal dichalcogenides (TMDs), metal oxides, phosphorene, silicene, germanene, and stanene, and all are under intensive investigation for their potential applications in nanoelectronic and optoelectronic devices[2–8].

Among those novel 2D materials, TMDs, TMDs, a honeycomb structure with single or few atomic layers, have attracted a lot of interest owing to their diverse electronic properties with semiconducting, metallic, or superconducting states[9–12]. By using the micro-mechanical cleavage method, Novoselov *et al.*[13] successfully synthesize the single layer MoS_2. Following the Novoselov's pioneering work, various TMDs, including WS_2, TiS_2, TiS_2, $TiSe_2$, $MoSe_2$, $TaSe_2$, $NbSe_2$ and $NiTe_2$, were gradually unraveled[14–24]. However, most of the pristine TMDs are intrinsically nonmagnetic, which hinders the utilization of these novel 2D nanosheets in the fields of spin-related nano-devices. Considerable efforts have been made to induce magnetism into these materials. For example, ferromagnetic characteristic has been detected in the MoS_2 nanoribbons, which is attributed to the presence of zigzag edge[25,26]. Zhou *et al.* showed that the magnetism of MoS_2 sheets can be tuned by embedding transition-metal atoms[27]. Chemical functionalization with hydrogen or fluorine is also an effective route to modify magnetic properties of TMDs[28–32]. Although these methods can induce magnetic behaviors in the 2D TMDs, it is difficult to control the edge structure and the doping/adsorption precisely in experiments. Therefore, developing a new type of TMDs materials with intrinsic magnetism in its pristine form is extremely urgent.

Recently, some ferromagnetic 2D monolayers containing 3d transition metal have been uncovered, such as FeC_2, CrN, δ-FeOOH and MnS_2[33–36]. Co is a typical 3d transition metal which has a Curie temperature Tc = 1405 K. Owing to the variable valence of Co, cobalt sulfides have diverse stoichiometric compositions such as CoS, CoS_2, Co_9S_8, and Co_3S_4[37–45]. Their thermal stability and electronic conductivity are usually better than other metal sulfides and have been considered promising materials in many fields. Nevertheless, to our knowledge, there has been no report about 2D monolayer of cobalt sulfides. In this work, using particle-swarm optimization (PSO) techniques combined with first-principles calculations, we firstly predict a new 2D monolayer composed of cobalt and sulfur atoms, Co_2S_2. The calculated results reveal that the Co_2S_2 nanosheet is both dynamically and thermodynamically stable, and is a ferromagnetic metal with estimated Curie temperature up to 404 K. Finally, we propose a possible way to synthesize it by chemical exfoliation from its parent three-dimensional (3D) $TlCo_2S_2$ crystal. Our finding greatly enriches the 2D families of transition metal sulfides.

[1]Department of Physics and Information Technology, Baoji University of Arts and Sciences, Baoji, 721016, China. [2]Department of Chemistry and Chemical Engineering, Baoji University of Arts and Science, Baoji, 721016, China. [3]Department of Applied Physics, Chongqing University, Chongqing, 400044, P.R. China. [4]Department of Physics, Southern University of Science and Technology, Shenzhen, Guangdong, 518055, China. Correspondence and requests for materials should be addressed to X.G. (email: xgu@cqu.edu.cn) or L.H. (email: huangl@sustc.edu.cn)

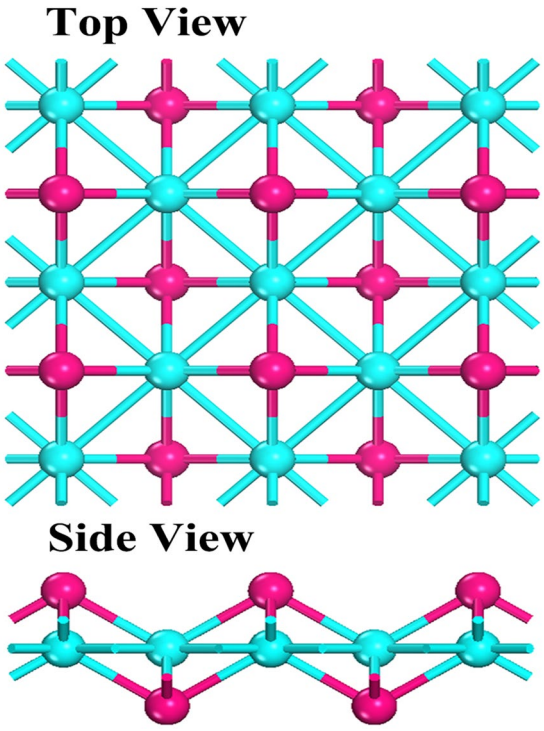

Figure 1. The top and side view of the 2D tetragonal structures of Co_2S_2. Purple and blue balls represent S and Co atoms, respectively.

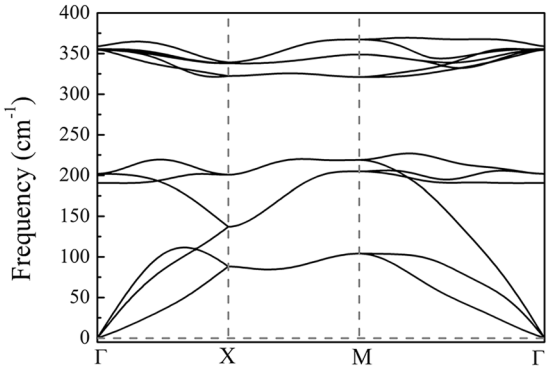

Figure 2. Calculated phonon dispersion along the high symmetry directions for the Co_2S_2 monolayer.

Results

The most stable structure of 2D cobalt sulfide is identified after 30 generations of searching. Figure 1 presents the top and side view of the optimized structure of Co_2S_2 monolayer, which crystallizes in the tetragonal space group, P4/nmm (No. 129), with each Co atom bonding with four S atoms and four Co atoms, and each S atom binding with four Co atoms. The unit cell of 2D Co_2S_2 monolayer contains two Co and two S atoms, and the optimized lattice parameters a = b = 3.638 Å. The structure of Co_2S_2 can be viewed as a single-layer PbO-type structure, in which cobalt atomic layer is sandwiched between the top and bottom sulfur atomic layers. The thickness of Co_2S_2 monolayer is 2.40 Å, and the bond lengths of Co-S and Co-Co are 2.182 Å and 2.572 Å, respectively.

To evaluate the stability of Co_2S_2 monolayer, we first calculate the average cohesive energy: $E_{coh} = (2E_{Co} + 2E_S - E_{Co_2S_2})/4$, where E_{Co}, E_S, and $E_{Co_2S_2}$ are the total energies of Co atom, S atom and one Co_2S_2 unit cell, respectively. The Co_2S_2 monolayer has a cohesive energy of 4.69 eV/atom, which is comparable to that of silicene (3.71 eV/atom), Cu_2Si (3.46) and Be_2C (4.86 eV/atom) at the same theoretical level[46,47]. The relatively large cohesive energy suggests that the Co_2S_2 monolayer is a strongly bonded network.

The key criteria for mechanical stability of a crystal are that the strain energy must be positive, which for a mechanically stable sheet would satisfy the following criteria[48,49]: $C_{11} > 0$, $C_{12} > 0$, $C_{44} > 0$, C_{11}-$C_{12} > 0$. The 2D elastic constants are calculated to be: $C_{11} = 106.2$ N/m, $C_{12} = 37.5$ N/m, and $C_{44} = 34.4$ N/m, indicating that the Co_2S_2 monolayer has robust mechanical stability.

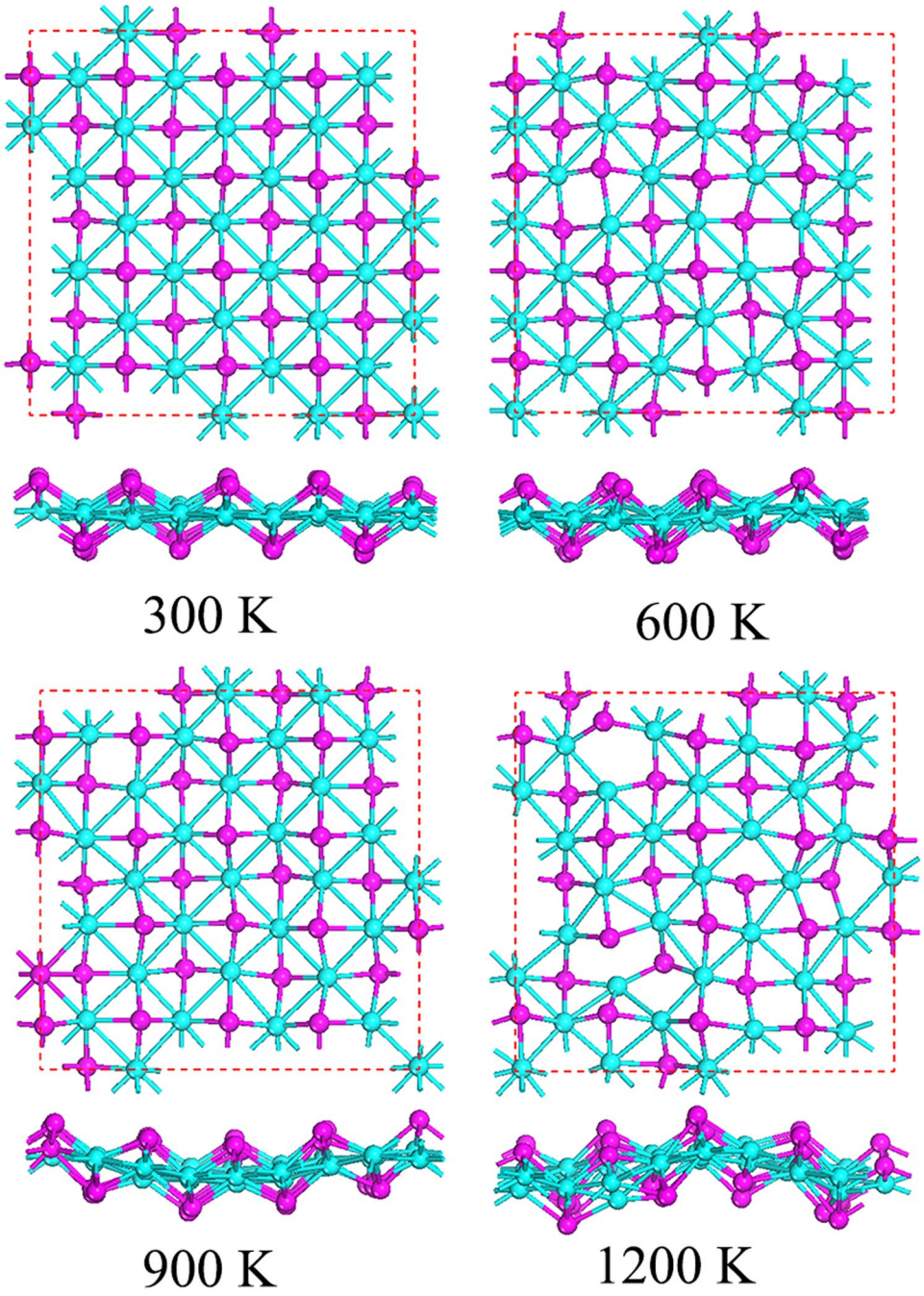

Figure 3. Structure snapshots of Co_2S_2 monolayer for AIMD simulation from 300 to 1200 K.

To further verify the structural stability of Co_2S_2 monolayer, we then calculate the phonon dispersion along the high-symmetry lines in the first Brillouin zone by using the Phonopy code. As shown in Fig. 2, the phonon spectrum shows no negative frequency in the whole Brillouin zone, which suggests Co_2S_2 monolayer is a stable phase without any dynamical instability. We also perform Ab initio molecular dynamics (AIMD) simulations to estimate the thermodynamical stability of 2D structure. Structure snapshots of Co_2S_2 monolayer taken at the end of each simulation are shown in Fig. 3. The results show that Co_2S_2 monolayer can maintain its structural integrity even up to 900 K. However, at the extremely high temperature of 1200 K, the planar structure is disrupted, indicating that 2D Co_2S_2 monolayer has good stability above the room temperature.

With the confirmed stability of the optimized monolayer Co_2S_2, we now turn to study the magnetic properties of Co_2S_2 monolayer. To explore the preferable magnetic ground state of Co_2S_2 monolayer, we construct three different initial magnetic configurations (i.e. FM, antiferromagnetic-1 (AFM1) and antiferromagnetic-2 (AFM2) states) in a 2×2 supercell, as shown in Fig. 4(a–c). The FM configuration is found to be 528 and 334 meV lower in energy than the AFM1 and AFM2 configurations per supercell, respectively, clearly indicating that FM state is the ground state of the Co_2S_2 monolayer, with a magnetic moment of 0.53 μB and 0.02 μB on each Co and S atom,

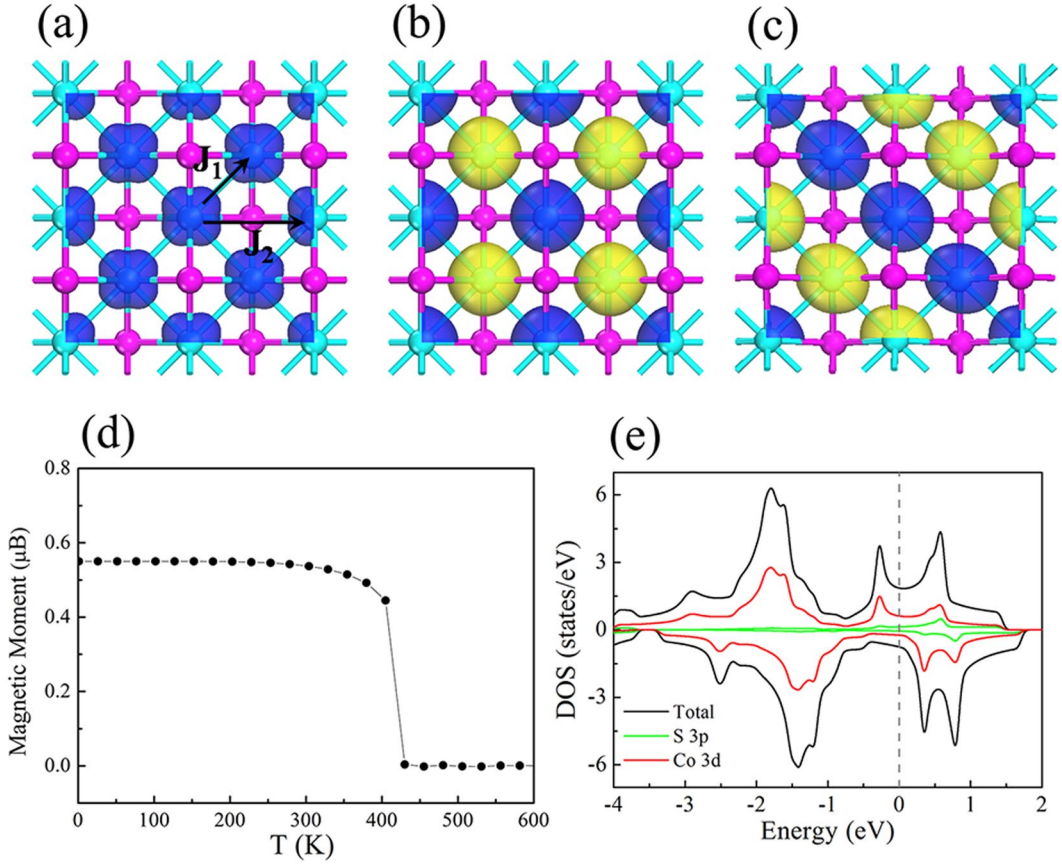

Figure 4. Spin density isosurface with a value of 0.01 e/Å3 for the FM (**a**), AFM1 (**b**) and AFM2 (**c**) coupling configurations of the Co_2S_2 monolayer. Blue and yellow indicate the positive (spin up) and negative (spin down) value, respectively. (**d**) Variation of the magnetic moment per Co atom with temperature. (**e**) The total DOS and PDOS for Co's 3d and S's 3p orbitals.

respectively. We further calculate the magnetic anisotropy energy (MAE), and find that the easy axis is perpendicular to the c-axis with a MAE of 0.17 meV per Co atom.

To gain an insight into the magnetic properties of Co_2S_2 monolayer, we also calculated the total density of states (DOS) and the atomic site projected density of states (PDOS). As shown in Fig. 4(e), Co_2S_2 monolayer is a FM metal. We find that Co 3d orbitals have a significance contribution to the DOS around the Fermi level. There is noticeable hybridization between Co 3d states and S 3p states in both the spin up and down channels near the Fermi level, which demonstrates that the S 3p orbitals play a key role in the FM coupling of the Co_2S_2 monolayer.

Considering the practical application of 2D Co_2S_2 monolayer, it is quite interesting to know if its Curie temperature is comparable to or higher than room temperature. To this end, we use Monte Carlo simulation based on a simplified Ising model, $H = -\sum_{i,j} J_{i,j} M_i \cdot M_j$, where $J_{i,j}$ is the nearest-neighbor exchange parameter and M is the local magnetic moment of Co atom. For simplicity, only two types of interactions in the Ising model are taken into account, i.e. the nearest-neighbor exchange parameter (J_1) and the next-nearest-neighbor exchange parameter (J_2), as shown in Fig. 4(a). Thus the expression for the exchange parameters for our system are $J_1 = \frac{E_{AFM_1} - E_{FM}}{32M^2}$ and $J_2 = \frac{2E_{AFM_2} - E_{FM} - E_{AFM_1}}{64M^2}$, where E_{FM}, E_{AFM_1} and E_{AFM_2} represent the total energy of FM, AFM_1 and AFM_2 states, respectively. The factor (1/32) is due to the double counting of the exchange interaction of 4 nearest-neighbor and 4 next-nearest-neighbor atoms in the summation. Substituting $E_{AFM_1} - E_{FM}$, $E_{AFM_2} - E_{FM}$ and M into the formula, we get $J_1 = 58.7$ and $J_2 = 15.8$ meV, respectively (See the Supplementary Information for details). During the Monte Carlo simulation, we use a 50×50 supercell to reduce the periodic constraints[50]. For each temperature the total number of Monte Carlo steps was 30000, allowing an initial relaxation time of 5000 steps and then sampling every 50 steps. Through Monte Carlo simulations, the variations of magnetic moment with respect to temperature are calculated. As shown in Fig. 4(d), the estimated T_C value is about 404 K, which is much higher than room temperature, implying that the Co_2S_2 monolayer has a robust ferromagnetism.

Although the newly predicted 2D Co_2S_2 monolayer shows intriguing structural and magnetic properties for potential applications in spin-related nano-devices, how to synthesize this material is a critical issue. We note that there is a bulk material $TlCo_2S_2$[51–53], in which the Co-S and Tl atomic layers are alternatively stacked in the z-direction, as shown in Fig. 5(a). It is interesting to note that the structure of 2D Co_2S_2 monolayer is exactly the same as the Co-S layer of bulk $TlCo_2S_2$. It is well-known that the monolayer MXenes can be chemically exfoliated from chemically bonded MAX phases. Hence, the Co_2S_2 layers could be exfoliated from the $TlCo_2S_2$ bulk

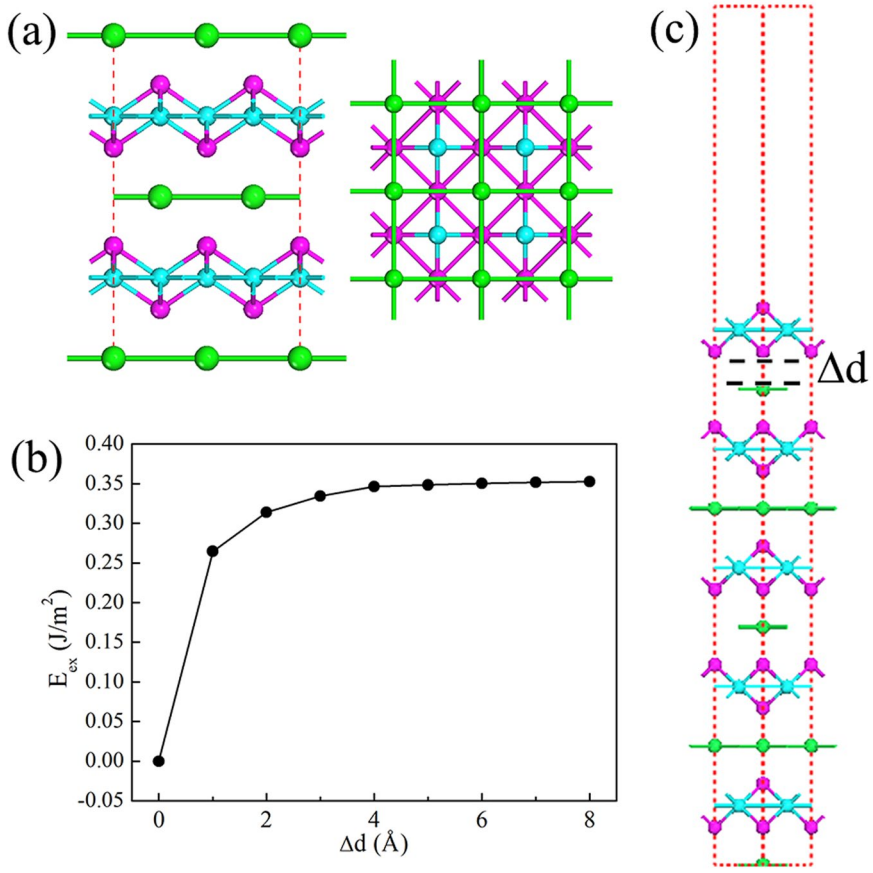

Figure 5. (**a**) Bulk phase of $TlCo_2S_2$, (**b**) Exfoliation energy E_{ex} as a function of the separation between the top layer and the rest of a five layered $TlCo_2S_2$ slab, (**c**) A five layered $TlCo_2S_2$ slab used to simulate the exfoliation procedure. Green, Purple and blue balls represent Tl, S and Co atoms, respectively.

by using the similar chemical exfoliation method[54]. Before measure the feasibility of exfoliating a Co_2S_2 monolayer from the bulk $TlCo_2S_2$, we revisit the $TlCo_2S_2$ bulk to test the quality of method that we used. The optimized lattice parameters of $TlCo_2S_2$ bulk are a = b = 3.73 Å, c = 13.00 Å, respectively. The FM configuration is found to be energetically more favorable than the AFM one by an energy difference of 155 meV, and the magnetic moment of Co atom is 0.83 μB. Our results are in good agreement with previous results[51,53]. Then we simulate the exfoliation procedure as gradually increasing the separation between the top Co_2S_2 layer and the rest of a five layered $TlCo_2S_2$ slab, as shown in Fig. 5(c). To estimate the exfoliation feasibility, the exfoliation energy is defined as $E_{ex} = E_{Co_2S_2} + E_{(TlCo_2S_2)_4+Tl} - E_{(TlCo_2S_2)_5}$. During the geometry relaxation, the bottom two layers are fixed. As shown in Fig. 5(b), the total energy is seen to increase with separation Δd at first, and then slowly converges to a fixed value 0.35 J/m^2, which is the energy (i.e. exfoliation energy E_{ex}) have to be overcome under exfoliation of a Co_2S_2 monolayer from the bulk crystal. The calculated exfoliation energy is very close to that of the well-known graphite (0.35 J/m^2)[55], which directly demonstrates that a Co_2S_2 monolayer might be exfoliated from the bulk $TlCo_2S_2$.

Discussion

By means of density functional theory (DFT) computations and global minimum search using particle-swarm optimization (PSO) method, we predict a new 2D cobalt sulfide monolayer, namely Co_2S_2, in which one Co layer is sandwiched by two S layers. Dynamical stability is predicted by the absence of any imaginary phonon modes. Molecular dynamics simulations show that this material can maintain its structural integrity at least up to 900 K. Magnetic studies and electronic structure calculations show that Co_2S_2 monolayer is a ferromagnetic metal with a high T_C up to 404 K. Finally, we propose that the Co_2S_2 monolayer can be synthesized be chemically exfoliated from bulk $TlCo_2S_2$ phase. Our findings greatly enrich the 2D families of transition metal sulfides.

Methods

The first-principles calculations are performed based on the density-functional theory (DFT) implemented in Vienna ab initio simulation package (VASP)[56,57]. The exchange-correlation potential is treated in the generalized-gradient approximation (GGA) of Perdew-Burke-Eznerhof (PBE)[58]. We use the projector augmented wave (PAW) method for the description of the electron–ion interaction. The energy cutoff for the plane wave basis expansion is set to 520 eV. The k-point sampling uses the Monkhorst-Pack scheme and employs 40 × 40 × 1 and 40 × 40 × 8 mesh for Co_2S_2 sheet and $TlCo_2S_2$ crystal, respectively[59]. The vacuum thickness along the z axis

is set 15 Å, which is enough to avoid the interaction between adjacent layers. For geometry optimization, all the internal coordinates are fully relaxed until the Hellmann-Feynman forces are less than 0.01 eV/Å. The phonon band structure of Co_2S_2 monolayer is calculated by using a finite displacement approach through the PHONOPY program[60]. The supercell of 4×4 original cell was adopted in the phonon calculation. Ab initio molecular dynamics (AIMD) simulations with canonical ensemble (NVT) at the temperature of 300, 600, 900, and 1200 K are performed with a time step of 1 fs in 5 ps, respectively. A supercell containing 4×4 unit cells is adopted as the model. 2D structure search is performed by using the particle-swarm optimization (PSO) method as implemented in the CALYPSO code[61,62]. During the structure search processes, the 60% structures of each generation (contains 30 structures) with lower enthalpies were selected to generate the structures for the next generation by PSO operation, and the other structures in new generation were randomly generated to increase the structural diversity. The number of generation is set to be 30. Usually, the structure searching simulation was stopped after 600~900 structures generated (20~30 generations). The ratio of cobalt and sulfur is fixed to 1:1, and the chemical formula ranges from Co_1S_1 to Co_4S_4 are considered. The local optimizations during the PSO simulation are performed using VASP. The MAE is obtained by applying the torque approach which has been proved to be an effective method for the reliable determination of MAE[63,64]. In this method, the MAE is expressed as

$$MAE = \sum_{i \in occ} \left\langle \psi_i \left| \frac{\partial H_{SO}}{\partial \theta} \right| \psi_i \right\rangle_{\theta=45^\circ} \quad (1)$$

where θ is the polar angle away from the molecular axis for spin momentum, ψ_i is the relativistic eigenvector, and H_{SO} is the SOC Hamiltonian.

References

1. Novoselov, K. S. *et al*. Electric field effect in atomically thin carbon films. *Science* **306**, 666–669 (2004).
2. Nag, A. *et al*. Graphene analogues of BN: novel synthesis and properties. *ACS Nano* **4**, 1539–1544 (2010).
3. Zeng, Z. *et al*. Single-Layer Semiconducting Nanosheets: High-yield preparation and device fabrication. *Angew. Chem. Int. Ed.* **50**, 11093–11097 (2011).
4. Vogt, P. *et al*. Silicene: compelling experimental evidence for graphenelike two-dimensional silicon. *Phys. Rev. Lett.* **108**, 155501 (2012).
5. Zhao, G. *et al*. Synthesizing MnO_2 nanosheets from graphene oxide templates for high performance pseudosupercapacitors. *Chem. Sci.* **3**, 433–437 (2012).
6. Huang, X., Zeng, Z. & Zhang, H. Metal dichalcogenide nanosheets: preparation, properties and applications. *Chem. Soc. Rev.* **42**, 1934–1946 (2013).
7. Liu, H. *et al*. Phosphorene: an unexplored 2D semiconductor with a high hole mobility. *ACS Nano* **8**, 4033–4041 (2014).
8. Balendhran, S., Walia, S., Nili, H., Sriram, S. & Bhaskaran, M. Elemental analogues of graphene: silicene, germanene, stanene, and phosphorene. *Small* **11**, 640–652 (2015).
9. Mak, K. F., Lee, C., Hone, J., Shan, J. & Heinz, T. F. Atomically thin MoS_2: a new direct-gap semiconductor. *Phys. Rev. Lett.* **105**, 136805 (2010).
10. Lukowski, M. A. *et al*. Enhanced hydrogen evolution catalysis from chemically exfoliated metallic MoS_2 nanosheets. *J. Am. Chem. Soc.* **135**, 10274–10277 (2013).
11. Acerce, M., Voiry, D. & Chhowalla, M. Metallic 1T phase MoS_2 nanosheets as supercapacitor electrode materials. *Nat. Nanotech.* **10**, 313–318 (2015).
12. Costanzo, D., Jo, S., Berger, H. & Morpurgo, A. F. Gate-induced superconductivity in atomically thin MoS_2 crystals. *Nat. Nanotech.* **11**, 339–344 (2015).
13. Novoselov, K. *et al*. Two-dimensional atomic crystals. *P. Natl. Acad. Sci. USA* **102**, 10451–10453 (2005).
14. Thomalla, M. & Tributsch, H. Photosensitization of nanostructured TiO_2 with WS_2 quantum sheets. *J. Phys. Chem. B* **110**, 12167–12171 (2006).
15. Hu, K. H., Hu, X. G., Xu, Y. F. & Pan, X. Z. The effect of morphology and size on the photocatalytic properties of MoS_2. *React. Kinet. Mech. Catal.* **100**, 153–163 (2010).
16. Splendiani, A. *et al*. Emerging photoluminescence in monolayer MoS_2. *Nano Lett.* **10**, 1271–1275 (2010).
17. Altavilla, C., Sarno, M. & Ciambelli, P. A Novel Wet Chemistry Approach for the Synthesis of Hybrid 2D Free-Floating Single or Multilayer Nanosheets of MS_2@oleylamine (M = Mo, W). *Chem. Mater.* **23**, 3879–3885 (2011).
18. Coleman, J. N. *et al*. Two-dimensional nanosheets produced by liquid exfoliation of layered materials. *Science* **331**, 568–571 (2011).
19. Feng, J. *et al*. Metallic few-layered VS_2 ultrathin nanosheets: high two-dimensional conductivity for in-plane supercapacitors. *J. Am. Chem. Soc.* **133**, 17832–17838 (2011).
20. Radisavljevic, B., Radenovic, A., Brivio, J., Giacometti, I. V. & Kis, A. Single-layer MoS_2 transistors. *Nat. Nanotech.* **6**, 147–150 (2011).
21. Feng, J. *et al*. Giant moisture responsiveness of VS_2 ultrathin nanosheets for novel touchless positioning interface. *Adv. Mater.* **24**, 1969–1974 (2012).
22. Chhowalla, M. *et al*. The chemistry of two-dimensional layered transition metal dichalcogenide nanosheets. *Nat. Chem.* **5**, 263–275 (2013).
23. Lin, C. *et al*. Hydrogen-incorporated TiS_2 ultrathin nanosheets with ultrahigh conductivity for stamp-transferrable electrodes. *J. Am. Chem. Soc.* **135**, 5144–5151 (2013).
24. Horzum, S. *et al*. Formation and stability of point defects in monolayer rhenium disulfide. *Phys. Rev. B* **89**, 155433 (2014).
25. Li, Y., Zhou, Z., Zhang, S. & Chen, Z. MoS_2 nanoribbons: high stability and unusual electronic and magnetic properties. *J. Am. Chem. Soc.* **130**, 16739–16744 (2008).
26. Ataca, C., Sahin, H., Akturk, E. & Ciraci, S. Mechanical and electronic properties of MoS_2 nanoribbons and their defects. *J. Phys. Chem. C* **115**, 3934–3941 (2011).
27. Zhou, Y., Su, Q., Wang, Z., Deng, H. & Zu, X. Controlling magnetism of MoS_2 sheets by embedding transition-metal atoms and applying strain. *Phys. Chem. Chem. Phys.* **15**, 18464–18470 (2013).
28. Ataca, C. & Ciraci, S. Functionalization of single-layer MoS_2 honeycomb structures. *J. Phys. Chem. C* **115**, 13303–13311 (2011).
29. Shi, H., Pan, H., Zhang, Y.-W. & Yakobson, B. I. Strong ferromagnetism in hydrogenated monolayer MoS_2 tuned by strain. *Phys. Rev. B* **88**, 205305 (2013).
30. Gao, D., Shi, S., Tao, K., Xia, B. & Xue, D. Tunable ferromagnetic ordering in MoS_2 nanosheets with fluorine adsorption. *Nanoscale* **7**, 4211–4216 (2015).
31. Manchanda, P., Sharma, V., Yu, H., Sellmyer, D. J. & Skomski, R. Magnetism of Ta dichalcogenide monolayers tuned by strain and hydrogenation. *Appl. Phys. Lett.* **107**, 032402 (2015).

32. Manchanda, P., Enders, A., Sellmyer, D. & Skomski, R. Hydrogen-induced ferromagnetism in two-dimensional Pt dichalcogenides. *Phys. Rev. B* **94**, 104426 (2016).
33. Chen, P. *et al.* Ultrathin nanosheets of feroxyhyte: a new two-dimensional material with robust ferromagnetic behavior. *Chem. Sci.* **5**, 2251–2255 (2014).
34. Kan, M., Adhikari, S. & Sun, Q. Ferromagnetism in MnX_2 (X = S, Se) monolayers. *Phys. Chem. Chem. Phys.* **16**, 4990–4994 (2014).
35. Zhang, S., Li, Y., Zhao, T. & Wang, Q. Robust ferromagnetism in monolayer chromium nitride. *Sci. Rep.* **4** (2014).
36. Zhao, T., Zhou, J., Wang, Q., Kawazoe, Y. & Jena, P. Ferromagnetic and Half-Metallic FeC_2 Monolayer Containing C2 Dimers. *ACS Appl. Mat. Interfaces* **8**, 26207–26212 (2016).
37. Kwon, S., Youn, S. & Min, B. Itinerant ferromagnetism in half-metallic CoS_2. *Phys. Rev. B* **62**, 357 (2000).
38. Gómez-Cámer, J., Martin, F., Morales, J. & Sanchez, L. Precipitation of CoS vs ceramic synthesis for improved performance in lithium cells. *J. Electrochem.Soc.* **155**, A189–A195 (2008).
39. Wang, Z., Pan, L., Hu, H. & Zhao, S. Co_9S_8 nanotubes synthesized on the basis of nanoscale Kirkendall effect and their magnetic and electrochemical properties. *CrystEngComm* **12**, 1899–1904 (2010).
40. Wang, Q. *et al.* CoS_2 hollow spheres: fabrication and their application in lithium-ion batteries. *J. Phys. Chem. C* **115**, 8300–8304 (2011).
41. Chen, G., Ma, W., Zhang, D., Zhu, J. & Liu, X. Shape evolution and electrochemical properties of cobalt sulfide via a biomolecule-assisted solvothermal route. *Solid State Sci.* **17**, 102–106 (2013).
42. Ko, Y. N., Choi, S. H., Park, S. B. & Kang, Y. C. Preparation of Yolk-Shell and Filled Co_9S_8 Microspheres and Comparison of their Electrochemical Properties. *Chem-Asian J.* **9**, 572–576 (2014).
43. Kong, S., Jin, Z., Liu, H. & Wang, Y. Morphological effect of graphene nanosheets on ultrathin CoS nanosheets and their applications for high-performance Li-ion batteries and photocatalysis. *J. Phys. Chem. C* **118**, 25355–25364 (2014).
44. Liu, S. *et al.* Controlled construction of hierarchical $Co_{1-x}S$ structures as high performance anode materials for lithium ion batteries. *CrystEngComm* **16**, 814–819 (2014).
45. Peng, S. *et al.* MS_2 (M = Co and Ni) Hollow Spheres with Tunable Interiors for High-Performance Supercapacitors and Photovoltaics. *Adv. Funct. Mater.* **24**, 2155–2162 (2014).
46. Li, Y., Liao, Y. & Chen, Z. Be_2C Monolayer with Quasi-Planar Hexacoordinate Carbons: A Global Minimum Structure. *Angew. Chem. Int. Ed.* **53**, 7248–7252 (2014).
47. Yang, L.-M. *et al.* Two-Dimensional Cu_2Si Monolayer with Planar Hexacoordinate Copper and Silicon Bonding. *J. Am. Chem. Soc.* **137**, 2757–2762 (2015).
48. Wang, J., Yip, S., Phillpot, S. & Wolf, D. Crystal instabilities at finite strain. *Phys. Rev. Lett.* **71**, 4182 (1993).
49. Cadelano, E. & Colombo, L. Effect of hydrogen coverage on the Young's modulus of graphene. *Phys. Rev. B* **85**, 245434 (2012).
50. Ležaić, M., Mavropoulos, P., Bihlmayer, G. & Blügel, S. Exchange interactions and local-moment fluctuation corrections in ferromagnets at finite temperatures based on noncollinear density-functional calculations. *Phys. Rev. B* **88**, 134403 (2013).
51. Huan, G., Greenblatt, M. & Ramanujachary, K. Magnetic ordering in metallic $TlCo_{2-x}Ni_xS_2$ ($0 \leq x \leq 2.0$) with the $ThCr_2Si_2$ structure. *Solid state Commun.* **71**, 221–228 (1989).
52. Greaney, M., Huan, G., Ramanujachary, K., Teweldemedhin, Z. & Greenblatt, M. Antiferro-to-ferromagnetic transition in metallic $TlCo_2S_xSe_{2-x}$ ($0 \leq x \leq 2.0$) with the $ThCr_2Si_2$ type structure. *Solid State Commun.* **79**, 803–810 (1991).
53. Ronneteg, S. *et al.* Magnetic and electronic structure of $TlCo_2S_2$. *J. Solid State Chem.* **177**, 2977–2984 (2004).
54. Liu, J., Sun, Q., Kawazoe, Y. & Jena, P. Exfoliating biocompatible ferromagnetic Cr-trihalide monolayers. *Phys. Chem. Chem. Phys.* **18**, 8777–8784 (2016).
55. Zacharia, R., Ulbricht, H. & Hertel, T. Interlayer cohesive energy of graphite from thermal desorption of polyaromatic hydrocarbons. *Phys. Rev. B* **69**, 155406 (2004).
56. Kresse, G. & Furthmüller, J. Efficiency of ab-initio total energy calculations for metals and semiconductors using a plane-wave basis set. *Comp. Mater. Sci.* **6**, 15–50 (1996).
57. Kresse, G. & Furthmüller, J. Efficient iterative schemes for ab initio total-energy calculations using a plane-wave basis set. *Phys. Rev. B* **54**, 11169 (1996).
58. Perdew, J. P., Burke, K. & Ernzerhof, M. Generalized gradient approximation made simple. *Phys. Rev. Lett.* **77**, 3865 (1996).
59. Monkhorst, H. J. & Pack, J. D. Special points for Brillouin-zone integrations. *Phys. Rev. B* **13**, 5188 (1976).
60. Togo, A. & Tanaka, I. First principles phonon calculations in materials science. *Scripta Mater.* **108**, 1–5 (2015).
61. Wang, Y., Lv, J., Zhu, L. & Ma, Y. Crystal structure prediction via particle-swarm optimization. *Phys. Rev. B* **82**, 094116 (2010).
62. Luo, X. *et al.* Predicting Two-Dimensional Boron–Carbon Compounds by the Global Optimization Method. *J. Am. Chem. Soc.* **133**, 16285–16290 (2011).
63. Wang, X., Wu, R., Wang, D. & Freeman, A. J. Torque method for the theoretical determination of magnetocrystalline anisotropy. *Phys. Rev. B* **54**, 61–64 (1996).
64. Hu, J. & Wu, R. Control of the magnetism and magnetic anisotropy of a single-molecule magnet with an electric field. *Phys. Rev. Lett.* **110**, 097202 (2012).

Acknowledgements

This work is supported by National Natural Science Foundation of China (No. 11704007, No. 11404160), Natural Science Basic Research plan in Shaanxi Province of China (No. 2016JM1016), Education Committee Natural Science Foundation in Shaanxi Province of China (No. 16JK1049), Young Talent fund of University Association for Science and Technology in Shaanxi Province of China (No. 20160233) and Baoji University of Arts and Sciences Key Research (Grant No. ZK16070). Computational support is provided by Supercomputing Cluster of Baoji University of Arts and Sciences.

Author Contributions

Y.Z. performed calculations and wrote the manuscript. J.M.P. and M.G.Z. discussed the results. X.G. and L.H. revised the paper.Y.Z. and J.M.P. contributed equally to this work.

Additional Information

Supplementary information accompanies this paper at https://doi.org/10.1038/s41598-017-16032-x.

Competing Interests: The authors declare that they have no competing interests.

Publisher's note: Springer Nature remains neutral with regard to jurisdictional claims in published maps and institutional affiliations.